Theoretical Studies on the Ground and Excited States of SO₃ Triatomic Molecule

AHMED M. MKADMH

Department of Chemistry, Aal-Aqsa University, P. O. Box 4051, Gaza Strip, Palestine
am.almagadma@alaqsa.edu.ps

Abstract: Density functional theory DFT (PBE0) with basis set aug-cc-pV(Q+d)Z has been used to compute molecular structures, electric dipole moments and hardnesses of ground and selected electronic excited states of sulfur trioxide. Vertical excitation energy and oscillator strength are given for each state at the same level of theory. With the use of the time-dependent TD-B3LYP/aug-cc-pVQZ approach, static linear and nonlinear optical (NLO) properties were studied. Ground state properties, excited states, and transition states were modeled using DFT/PBE0, CIS and CIS(D) and QST2 and QST3 respectively. Geometrical and electrical properties of ground and excited states have been presented. Four local minima structures of SO₃ were distinguished in addition to SO₃ (D₃ₕ) global minimum where the C_S symmetry square one is the least stable. CIS and CIS(D) calculations revealed insignificant variations in geometrical parameters among triplet and singlet excited states of the global minimum. It is observed that the state of minimum polarizability and hyperpolarizabilities is associated with the geometry of minimum energy content. The impact of symmetric stretching frequency on the mean dipole polarizability $\langle\alpha\rangle$ and anisotropy $\Delta\alpha$ of the global minimum isomer have been fitted to a fourth order Taylor series expansion. Our calculated

values of $\left(\dfrac{d^n\langle\alpha\rangle}{dR^n}\right)_e$ for $n = 1,2$ are $22.146\,e^2a_o^2E_h^{-1}$ and $10.026\,e^2a_o^2E_h^{-1}$ while those of $\left(\dfrac{d^n\langle\alpha\rangle}{dR^n}\right)_e$

are $19.764\,e^2a_o^2E_h^{-1}$ and $21.300\,e^2a_o^2E_h^{-1}$ respectively.

Introduction

The prototypical symmetric SO₃ is an important molecule both industrially and environmentally and thus has been a subject of theoretical and experimental interest at both ground and excited states[1-18]. In addition, it is of astronomical importance as a consequence of its presence on the planet Venus and Jupiter's moon Io[19,20].

Upon condensation of pure gaseous SO₃ molecule at 27 °C, a meta-stable colorless cyclic trimmer γ-SO₃, is formed which is eventually converted to the stable[21] fibrous α-SO₃. While oxidation of SO₂ leads ultimately to the production of sulfuric acid H₂SO₄, the photolysis of H₂SO₄ leads to the formation of SO₃ which, in turn, suffers further photolysis yielding SO₂ gaseous molecule[22].

Gaseous sulfur trioxide, one of the primary pollutants in the acid rain, is an aggressively hygroscopic, highly reactive oxidant and hypervalent triangular planar molecule with D_{3h} symmetry as predicted by Valence Shell Electron Pair Repulsion Model, electron diffraction studies and dielectric measurements[5,6]. Henfrey and Thrush have reported consistent vibrational spectra of SO_3 with the well established D_{3h} symmetry[7]. Geometrical data concluded by electron diffraction included 141.8 pm and 119.4 °C for S - O bond distance and OSO bending angle respectively[8,9]. Ortigoso *et al*. reported a value of 141.7 pm for the bond distance of the molecule in concern[10]. The shortness of the S-O bond distance is attributed to the back bonding overlap of oxygen pπ to the sulfur vacant dπ orbitals. The electronic ground state $\tilde{X}\,^1A_1$ of SO_3 molecule[22] has the electronic configuration $(core\,)^{16}\,6a_1^2\,7a_1^2\,3b_1^2\,8a_1^2\,2b_2^2\,9a_1^2\,4b_1^2\,10a_1^2\,5b_1^2\,1a_2^2\,6b_1^2\,11a_1^2\,4b_2^0\,12a_1^0\,7b_1^0\ldots..$ It has 8 core molecular orbitals and 16 valence MO's; 12 occupied and 4 virtual with the minimal basis set calculation since the number of virtual orbital is basis set dependent.

SO_3 has six vibrational degrees of freedom, giving rise to four fundamental vibrational modes assigned as S - O symmetric stretching $\nu_1\left(a_1'\right)=1065\ cm^{-1}$, out of plane bending $\nu_2\left(a_2''\right)=498\ cm^{-1}$, doubly degenerate antisymmetric in-plane S-O stretching $\nu_3\left(e'\right)=1391\ cm^{-1}$ and doubly degenerate in-plane bending $\nu_4\left(e'\right)=530cm^{-1}$; symbol in parentheses indicate the symmetry class of the given vibrational mode[4,10]. The fundamental vibrational modes ν_2 ν_3 and ν_4, along with several hot bands were intensively investigated by Msiello *et al.* by the means of High Resolution Infrared Spectroscopy and Coherent anti-Stokes Raman Scattering Spectroscopy[2-4,11,12].

Harmonic frequencies, in addition to geometry and heat of atomization of SO_3, were investigated theoretically by Martin using coupled cluster with single, double, and perturbed triple excitation with Martine-Taylor basis set (CCSD(T)/MTcore). The values of the bond distance, atomization energy and the four vibrational fundamentals reported by Martin are 141.8 pm, 335.96 kcal mol^{-1} and ν_1 = 1082.7 cm^{-1}, ν_2 = 502.6 cm^{-1}, ν_3 = 1415.4 cm^{-1}, ν_4 = 534.0 cm^{-1} respectively[13,14]. Infrared absorption of SO_3 in solid Ar conducted by Lee *et al.* gives the lines[15] at 2438.7, 1385.2, 5270.1 and 490.3 cm^{-1}, which are in good agreement with those reported by Bondybey and English[16]. These lines are assigned as $\nu_1\left(a_1'\right)+\nu_3\left(e'\right)$, $\nu_3(e')$, $\nu_4(e')$ and $\nu_2\left(a_2'\right)$, respectively.

Excited states of SO_3 have been repeatedly considered as well as its ground states. The absorption spectrum has been assigned in the visible to vacuum-ultraviolet region where the electronic bands were found to be centered at 148 nm with a maximum cross section of 3.6×10^{-17} cm^2 molec^{-1} about 1.0×10^{-17} cm^2 molec^{-1} larger than earlier measurements[17,18]. Vertical excitation energies and oscillator strengths of the lowest energy electronic transitions of SO_3 were studied theoretically by Robinson *et al.* who found that the electronic transitions of SO_3 calculated with the multireference configuration interaction (MRCI) method are consistent with the experimental results[22]. The electric dipole moment of a molecule plays a crucial role in structural chemistry. This parameter is expected to have different values in different excited states, due to possible changes in nuclear rearrangements and redistribution of electron charge density.

When a molecule is subjected to an external electric field *E* the molecular charge density may rearrange, hence the dipole moment may changes. The influence on the dipole moment could be described mathematically by equation (1)[23]:

$$\mu_{e,j}(E) = \mu_{e,j}(o) + \sum_{j=x}^{z} \alpha_{ij} E_j + \frac{1}{2!}\sum_{j=x}^{z}\sum_{k=x}^{z} \beta_{ijk} E_j E_k + \frac{1}{3!}\sum_{j=x}^{z}\sum_{k=x}^{z}\sum_{t=x}^{z} \gamma_{ijkt} E_j E_k E_t + ... \quad (1)$$

Here μ_e, j is the jth Cartesian component of the dipole moment, μ_e, j(O) is the dipole in the absence of a field and μ_e, j (E) is the dipole moment in the presence of a field. The nine independent quantities α_{ij} define the dipole polarizability tensor and β_{ijk} and γ_{ijkl} are the first and the second members of an infinite number of dipole hyperpolarizability tensors. While γ occurs for both centrosymmetric and non-centrosymmetric media, β vanishes for centrosymmetric groups. One would notice a weak component β_μ directed along the applied electric field for systems with $\beta \neq 0$ defined as β_{vec}[24]. The average molecular polarizability $<\alpha>$, anisotropy $\Delta\alpha$ and average hyperpolarizabilities β and γ descriptors are calculated utilizing the following expressions:

$$\langle\alpha\rangle = \frac{1}{3}\sum_{i=x}^{z}\alpha_{ii} \tag{2}$$

$$\Delta\alpha = \frac{1}{\sqrt{2!}}\sum_{\substack{i=x,y \\ j=y,z}}\left(\alpha_{ii}-\alpha_{jj}\right)^2 \tag{3}$$

$$\langle\beta\rangle_{vec} = \left(\sum_{i=x}^{z}\beta_i^2\right)^{1/2} \tag{4}$$

$$\beta_{i=x,y,z} = \beta_{iii} + \frac{1}{3}\sum_{j\neq i}\left(\beta_{ijj}+2\beta_{jji}\right) \tag{5}$$

$$\gamma = \frac{1}{5}\sum_{\substack{i=x,y,z \\ j=x,y,z}}\gamma_{iijj} = \frac{1}{5}\left(\gamma_{xxxx}+\gamma_{yyyy}+\gamma_{zzzz}+2\left(\gamma_{xxyy}+\gamma_{yyzz}+\gamma_{zzxx}\right)\right) \tag{6}$$

Chemical hardness η is defined in terms of the theory of the density functional as the second derivative of the total electronic energy with respect to the number of electrons in the system while external potential is maintained constant[25]. Besides, η could be expressed in terms of vertical ionization energy and electron affinity in the form of energy gap between frontier orbitals; the highest occupied molecular orbital (HOMO) and the lowest unoccupied molecular orbital (LUMO) where[26], $\eta = \frac{(\varepsilon_{LUMO}-\varepsilon_{HOMO})}{2}$.

As a consequence of its multilateral importance and in extension to our previous[27] study of SO_2, ground and excited states of SO_3 will be investigated theoretically to provide more insight on its geometry, electrical and optical properties.

Computational details

Molecular geometry of the ground state SO_3 (D_{3h}) isomer was fully optimized with different density functionals (B3LYP[28,29], PBE0[30,31], MPW91[32] and LSDA[33]) in combinations with six different basis sets (6-311++G(3d,3pd), 6-311++G(3df,3pd), DGDZVPZ, SDD, aug-cc-pVQZ and aug-cc-pV(Q+d)Z) in attempt to assign the most appropriate functional/basis set combination for the calculations in this study. The static electronic polarizability of SO_3 (D_{3h}) isomer has been calculated as a numerical derivative of the dipole moment using the finite

field method[34] in the presence of a step-size 0.001 *au* electric field along the Cartesian axis at the same afore mentioned functional/basis set combinations utilizing the optimized wave functions. Furthermore, polarizability of SO_3 (D_{3h}) isomer has been computed with TD-B3LYP/aug-cc-pV(Q+d)Z where the fully optimized PBE0/aug-cc-pV(Q+d)Z extracted wave function has been used as the input data for polarizability calculations. The notation that will be used to represent that is TD-B3LYP/aug-cc-pV(Q+d)Z// PBE0/aug-cc-pV(Q+d)Z.

The generalized-approximation exchange-correlation functional of Perdew, Burke and Ernzerhof, PBE0[30,31], in combination with the sophisticated standard Dunning's correlation consistent quadruple-zeta augmented basis set with diffuse functions, aug-cc-pV(Q+d)Z[35], proved to be the most reliable choice of them to be employed in this study for geometrical optimizations unless otherwise stated. Thus molecular geometries of all structures involved in the study were fully optimized in the gas phase using internal coordinates at the PBE0/aug-cc-pV(Q+d)Z level of theory. Optimized geometries of all structures were confirmed to be minima on the potential energy surface as revealed by inexistence of imaginary frequencies. Energy calculations were performed with single point energy calculations utilizing the fully optimized geometries; PBE0/aug-cc-pV(Q+2df)Z// PBE0/ aug-cc-pV(Q+d)Z and then chemical hardness were calculated. Bond critical points were calculated using AIM2000[36], utilizing the Gaussian 09 extracted wave functions.

Transition structures between SO_3 isomers were examined using quadratic synchronous transit (QST2) with the same level of theory; PBE0/aug-cc-pV(Q+d)Z. On QST2 failure, quadratic synchronous transit-guided quasi-Newton approach (QST3) was the alternative where a first guess of the transition state was included. The stationary points were verified as first order saddle points and thus energy barriers between sulfur trioxide isomers were calculated. The reaction path was followed by means of internal reaction coordinate (IRC) with a maximum number of 20 points on each side of the path and step size 0.3 amu$^{-0.5}$ bohr where geometry is optimized at each point along the reaction path using the same aug-cc-pV(Q+d)Z basis set.

The lowest ten singlet and triplet excited states were optimized with the configuration interaction single-excitation CIS/aug-cc-pV(Q+d)Z and CIS(D)/aug-cc-pV(Q+d)Z methods in an iterative procedure until the lowest energy of desired excited states were determined[37,38].

Time-dependent density functional of Becke three-parameter hybrid functional of Lee, Yang and Parr[28,29], is employed to probe the static polarizability and the static first and second-order non linear optical NLO properties, TD-B3LYP/aug-cc-pV(Q+d)Z//PBE0/aug-cc-pV(Q+d)Z. All of the TD-B3LYP calculations have been carried out using Firefly modeling software[39]. The aug-cc-pV(Q+d)Z basis set for sulfur/oxygen corresponds to (17s,12p,5d,3f,2g)/(14s,8p,5d,4f,3g) primitive set contracted to [7s,6p,5d,3f,2g]/[7s,6p,5d,4f,3g] basis functions; (89 and 105 contracted base functions, respectively), adding up to 404 basis functions for the entire molecule.

Atomic charges were calculated using natural population analysis[40]. The impact of symmetric stretching frequency on linear optical susceptibility and anisotropy of the ground state global minima isomer was examined using PBE0/aug-cc-pV(Q+d)Z and B3LYP/aug-cc-pV(Q+d)Z level of theories around the equilibrium bond length (R_e) with $\Delta R = R_i - R_e = \pm$ 5.0 pm. The Gaussian 09 series[41] of programs employed for the *ab initio* calculations were run on an Intel(R)Core(TM)i7 PC.

Results and Discussion

Level of theory selection

All functional/basis set combinations predicted zero electric dipole moment and 120 ^{o} for the OSO bending angle of the ground state SO_3 (D_{3h}) isomer. Bond length and electric polarizability estimated are presented in Table 1. The bond distance prediction experienced significant variation with different functionals with the same basis set. PBE0 and MPW91 functionals with the sophisticated aug-cc-pvqz basis set provided S-O bond distance 142.3 pm and 142.2 pm respectively; 0.5 pm and 0.4 pm larger than the experimental value[8,9]. The S-O bond length was found to have magnitude of 141.78 pm at the two previously indicated functionals upon inclusion of the tight d function aug-cc-pV(Q+d)Z which in excellent agreement with experimental bond distance[8,9] predicted by both Bell *et al.*[42] and Martin[13]. Deviations in both cases from the experimental value have been almost completely eliminated.

Table 1. SO_3 global minima bond length in pm and polarizability in au at different functional/basis set combinations

Basis set	B3LYP		PBE0		MPW91		LSDA	
	d_{S-O}	$<\alpha>$	d_{S-O}	$<\alpha>$	d_{S-O}	$<\alpha>$	d_{S-O}	$<\alpha>$
6-311++G(3d,3pd)	142.8	27.943	142.1	27.338	142.1	27.313	142.9	28.571
6-311++G(3df,3pd)	142.5	27.805	141.8	27.225	141.8	27.192	142.5	28.459
DGDZVPZ	145.6	25.604	144.5	25.075	144.5	25.023	145.2	26.194
SDD	159.8	28.857	158.3	28.472	158.3	28.049	159.1	28.803
cc-pVQZ	143.1	26.642	142.3	26.133	142.2	25.248	143.2	24.493
cc-pV(Q+d)Z	142.5	26.344	141.8	25.858	141.7	25.785	142.5	26.989
Aug-cc-pVQZ	143.1	28.916	142.3	28.190	142.2	28.082	143.2	29.652
Aug-cc-pV(Q+d)Z	142.5	28.603	141.8	27.909	141.7	27.798	142.5	29.328

The same aforementioned functionals predicted a value of 28.190 au and 28.082 au with the aug-cc-pVQZ for the static polarizability where the first value is in excellent agreement with the experimental value (28.212 au)[43]. However, the inclusion of the tight d function slightly lowered polarizability invariant 27.909 au and 27.798 au with 1.07% and 1.47% deviation from the experimental value.

Bond distance and polarizability prediction by B3LYP and LSDA with all basis sets involved showed large deviation from the experimental values as it is obvious from Table 1. However, Deviations of $<\alpha>$ with B3LYP and LSDA were reduced from 2.50% and 5.10% to 1.39% and 3.96% respectively as a consequence of the addition of the d function to the basis set aug-cc-pvqz. Deviation in bond distance calculation with the same functional with aug-cc-pV(Q+d)Z basis set, showed tangible improvement where deviation from experimental value has been reduced from 1.0% to 0.5%.

It is found that the *S-O* bond length varied between 142.2 and 143.2 at the cc-pVQZ basis set with all functionals, which is larger than the experimental *S - O* bond distance 141.8 pm. The polarizability was found to have magnitude between 24.493 au and 26.642 au at the cc-pVQZ basis set, which is much less than the corresponding experimental polarizability 28.212 au.

The *S - O* bond length predicted by the PBE0/cc-pV(Q+d)Z is 11.84 pm, which is in excellent agreement with the experimental value. Yet, the polarizability that has been estimated at this level of theory (28.858 au) deviates largely from the experimental polarizability (8.3%). Similar results have been obtained by the MPW91/cc-pV(Q+d)Z level of theory.

The *S - O* bond distance estimation was 142.5 pm by the calculations conducted at the B3LYP/cc-pV(Q+d)Z and LSDA/ cc-pV(Q+d)Z level of theories, which is larger than the corresponding experimental value. The polarizability calculated value deviated by 1.39% and 3.96% at the same level of theories, respectively.

One more thing that could be remarked that the bond length prediction with each of PBE0/6-311++G(3df,3pd) and MPW91/6-311++G(3df,3pd) level of theories was in excellent agreement with that of the aug-cc-pV(Q+d)Z. To the contrary, <α> prediction was significantly lower-estimated with these level of theories.

It worth indicating that the geometrical parameters computed by PBE0/aug-cc-pV(Q+d)Z are exactly equal to those predicted by the large basis set aug-cc-pV(5+d)Z at the same DFT(PBE0) level of theory conducted by us as an extension to this work.

As a consequence of that the PBE0/aug-cc-pV(Q+d)Z level of theory will have been employed to fully optimize all isomers included in this study. The calculated electronic energies and zero point energies with all functional/basis set combinations are presented in the supplementary materials, Table 2.

Table 2. Ground state isomer electronic energy prediction by DFT functional

| Functional	Basis set	E+ZPE
PBE1PBE	6-31++G(3d,3pd)	-623.5197811
	6-311++G(3df,3pd)	-623.5411269
	DGDZVPZ	-623.4344158
	SDD	-623.1635228
	aug-cc-Pvqz	-623.5638681
	aug-cc-PV(Q+d)Z	-623.5764063
	aug-cc-pV(5+d)Z	-623.5801248
MPW1PW91	6-31++G(3d,3pd)	-623.8457362
	6-311++G(3df,3pd)	-623.8669347
	DGDZVPZ	-623.7609787
	SDD	-623.4898422
	aug-cc-Pvqz	-623.8898034
	aug-cc-PV(Q+d)Z	-623.9024298
B3LYP	6-31++G(3d,3pd)	-623.9037757
	6-311++G(3df,3pd)	-623.9187955
	DGDZVPZ	-623.8268057
	SDD	-623.5631239
	aug-cc-Pvqz	-623.9457893
	aug-cc-PV(Q+d)Z	-623.9582499
LSDA	6-31++G(3d,3pd)	-621.7868962
	6-311++G(3df,3pd)	-621.6667004
	DGDZVPZ	-621.7216187
	SDD	-621.4432769
	aug-cc-Pvqz	-621.826053
	aug-cc-PV(Q+d)Z	-621.8393282

As an extension to polarizability calculations, polarizability of SO3 (D$_{3h}$) has been computed with the Firefly software at the TD-B3LYP/aug-cc-pV(Q+d)Z utilizing the PBE0/aug-cc-pV(Q+d)Z wave function. The calculated value is 28.314 au which is in excellent agreement with the experimental value (28.212 au). Deviation in polarizability has

been reduced from 1.07% calculated with PBE0/aug-cc-pV(Q+d)Z//PBE0/aug-cc-pV(Q+d)Z to 0.4%. As a consequence of this result, polarizability and the NLO properties will have been calculated at the TD-B3LYP/aug-cc-pV(Q+d)Z level of theory with the Firefly software utilizing the wave function predicted by the PBE0/aug-cc-pV(Q+d)Z level of theory using the Gaussian 09 series of programs.

Vibrational calculations with the PBE0/aug-cc-pV(Q+d)Z which giving rise to four vibrational modes designed as symmetric stretching $v_1(a_1') = 1108.1 cm^{-1}$; IR inactive, out of plane bending $v_2(a_2'') = 509.4 cm^{-1}$, doubly degenerate antisymmetric stretching $v_3(e') = 1438.7 cm^{-1}$ and doubly degenerate bending $v_4(e') = 535.2 cm^{-1}$ were in good agreement with the corresponding experimental values and those have been predicted by Jou *et al.*[15] and Martin[13]. The corresponding infrared intensities of the estimated vibrational modes are 0.0 km mol^{-1}, 33.5 km mol^{-1}, 203.95 km mol^{-1} and 27.09 km mol^{-1} respectively.

Molecular structures of SO₃ isomers

Four different local ground state stationary isomers each with C_S point group symmetry in addition to the SO_3 (D_{3h}) one were located, as illustrated in Figure 1. The D_{3h}, cis and trans isomers are planar, whereas the others are nonplanar. Obviously, the d_{O-O} = 148.9 pm and 144.9 pm in the nonplanar isomers (cyclic and square) are longer than those of the planar ones (d_{O-O} = 130.4 pm, 132.1 pm and 141.8 pm in the cis, trans and SO_3 (D_{3h}) isomers respectively). Additionally, two different S-O types were predicted in the planar isomers; the central one about 157.5 pm is remarkably longer than the terminal ones (143.4 pm in the cis and 143.7 pm in the trans isomers).
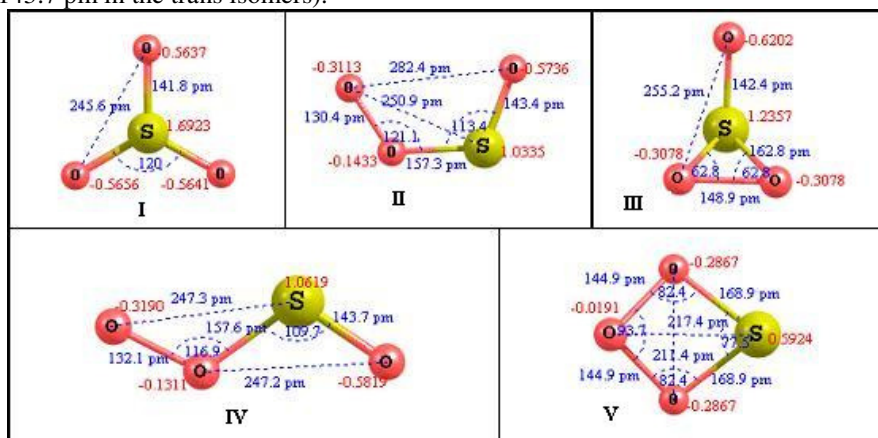
Figure 1. Predicted isomers of sulfur trioxide with their geometrical parameters and atomic charges at PBE0/aug-cc-pV(Q+d)Z level of theory; bond distances and bending angles are given in blue colors in *pm* and angles respectively, while Mulliken charges are depicted in red one in coulomb (*Colors will be visible only in the online version*)

Energy of SO₃ isomers

While the SO_3 (D_{3h}) isomer proved to be global minimum; E = -623.5801248 au, the square isomer is the least stable; 158.29 kcal mol^{-1} higher than the global minimum. The cis isomer lies approximately 5.58 kcal mol^{-1} lower than the trans and 25.00 kcal mol^{-1} more energetic than the cyclic one. Energy of isomers relative to the most stable SO_3 (D_{3h}) isomer (in terms

of stability) is: D_{3h} SO_3 < cyclic (64.60 kcal mol^{-1}) < cis 89.60 kcal mol^{-1} < trans (95.17 kcal mol^{-1}) <square (158.29 kcal mol^{-1}). The same trend is obtained using B3LYP/aug-cc-pV(Q+d)Z, almost with energy difference very close to the one aforementioned.

It is found that the total energy of each isomer is larger than the energy sum of its constituent monomers. Binding energies of the isomers that computed relative to the separated monomers and corrected for vibrational zero-point energies are in the following order:

SO_3 (D_{3h}) (153.12 kcal mol^{-1}) > cyclic (88.52 kcal mol^{-1}) > cis (63.52 kcal mol^{-1}) > trans (57.94 kcal mol^{-1}) > square (-5.17 kcal mol^{-1}) > energy of SO_2 +O. Energy calculations have reflected a relative high instability of the square isomer and thus higher activity and lower hardness than the other ground state isomers. The hardness order of the isomers is; SO_3 (D_{3h}) (3.7081 *eV*) > cyclic (3.4719 *eV*) > cis (1.8535 *eV*) > trans (1.6073 *eV*) > square (1.5828 *eV*). Potential extrema $V_{S,min}$ and $V_{S,max}$ on the molecular surface electrostatic potential (MSEP) of the isomers have been estimated using MOLEKEL:5.1[45], utilizing the Gaussian 09 generated wavefunctions. The calculated v_S, min values (red regions) were located at oxygen ranging from -32.88 kcal mol^{-1} for the SO_3 (D_{3h}) isomer to -58.80 kcal mol^{-1} for the cis one. The lower potential value would provide suitable site of attack by incoming electrophile as a proton, for instance. The higher potential values $V_{S,max}$ were found associated with the sulfur site, providing optimized site for nucleophilic attack, ranging from 53.58 kcal mol^{-1} for square isomer to 95.33 kcal mol^{-1} for the cyclic one. This is in accordance with the bond critical point (BCP) calculations conducted using AIM2000 program software. BCPs were shifted toward higher potential sites in all isomers reflecting higher electron density at the more electronegative oxygen atoms**.** Figure 2 provides the molecular graphs of the D_{3h}, cis and the square isomers where the BCPs denoted as large red dots along the bonds baths constituting the molecular graphs. Obviously, BCPs act as gateways between bonded atoms where the charge densities reach maxima along the planes tangential to the interaction surfaces and minima along the orthogonal directions. One important comment emanating from the Figures 2 II and 2 III is that the bond baths are not necessarily straight lines due to the significant curvatures in S-O bond baths. These curved bond baths are consistent with the concept of bonds strain.
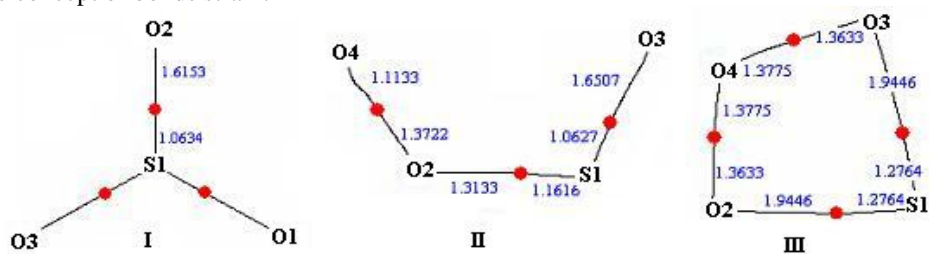
Figure 2. Molecular graphs for the D_{3h}, cis and square isomers in their equilibrium geometries. Bond critical points (BCPs) are denoted as large red dots. Numbers refer to the length of the gradient path along the BCPs

Energy barriers

Rotational energy barrier ΔE_b in kcal mol^{-1} is estimated as the energy difference between the isomer and the corresponding transition state. For instance ΔE_b between the cyclic isomer and the TS6 is 33.02 kcal mol^{-1}**,** while the corresponding ΔE_b between TS6 and D_{3h} is 97.62 kcal mol^{-1}**.** All these calculations are corrected to zero point energy calculations. Figure 3 roughly depicts the DFT estimated energy profile of the isomers and the transitions among them.
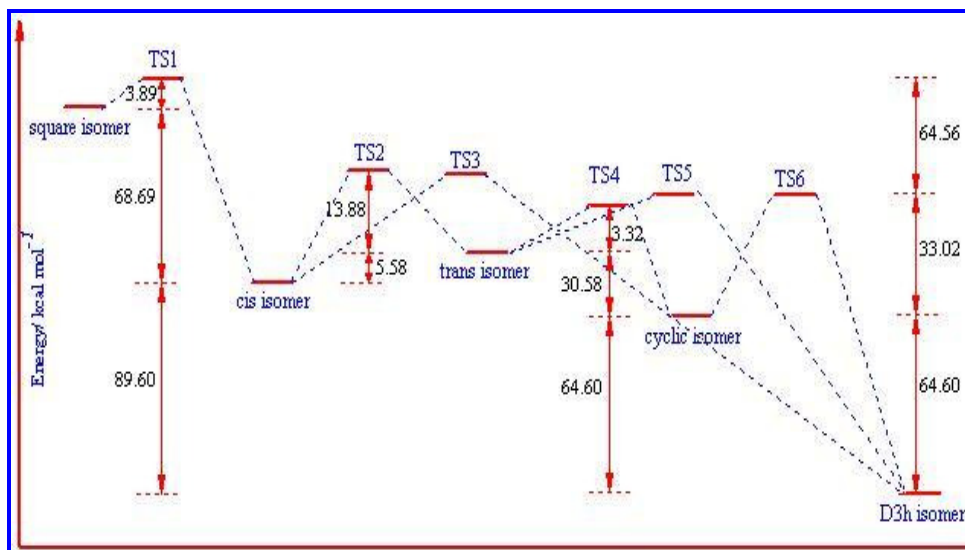
Figure 3. Energy profile of SO_3 isomers where TS stands for the transition energy as predicted by PBE0/ aug-cc-pV(Q+2df)Z //PBE0/aug-cc-pV(Q+d)Z level of theory.

Table 3 reports energy barriers, vibrational wave numbers, polarizabilities, anisotropies and hardnesses of the predicted transition states. The average polarizability is given in atomic units $e^2 a_o^2 E_h^{-1}$ which approximately equal $1.649 \times 10^{-41} c^2 m^2 J^{-1}$, equivalent to 1.482×10^{-25}. Units of β is $e^3 a_o^3 E_h^{-2}$, equivalent to $3.206 \times 10^{-53} c^3 m^3 J^{-2}$, units of γ is $e^4 a_o^4 E_h^{-3}$, equivalent to $6.235 \times 10^{-65} c^4 m^4 J^{-3}$ and the atomic unit of the electric dipole moment μ is D (debye), equivalent to 3.336x10-30 cm. Predicted energies, zero point energies, hardnesses and energies and energy gaps between frontier orbitals are tabulated in supplementary materials (Table 4).

Table 3. Energy barrier ΔE_b in kcal mol^{-1}, v in cm^{-1}, $<\alpha>$, $\Delta\alpha$ in *au*, η in *eV* and μ in D

Transition state		ΔE_b	v	$<\alpha>$	$\Delta\alpha$	η	μ
TS1	Square	3.89	-288.0	32.714	9.422	1.3842	1.5349
	Cis	72.58					
TS2	Cis	19.46	-653.9	36.698	21.316	1.3978	3.5167
	Trans	13.88					
TS3	Cis	8.02	-979.8	34.934	14.973	0.9826	1.4454
	SO_3	97.62					
TS4	Trans	3.32	-324.3	37.909	27.247	1.4908	2.418
	Cyclic	33.89					
TS5	Trans	2.45	-980.7	34.941	5.500	0.9815	1.4419
	SO_3	94.91					
TS6	Cyclic	35.88	-980.1	34.942	8.045	0.9818	1.4434
	SO_3	97.62					

Table 4. Energy (*E*) in au, zero point energy (*ZPE*) in au, energy of the highest occupied molecular orbital (E_{HOMO}) in (*eV*), energy of the lowest occupied molecular orbital (E_{LUMO}) in (*eV*) and energy gap between frontier orbitals ($\Delta E = |E_{HOMO} - E_{LUMO}|$) in (*eV*) of the SO_3 isomers and transition states along the reaction coordinates estimated by PBE0/aug-cc-pV(Q+2df)Z //PBE0 /aug-cc-pV(Q+d)Z

Isomer	*E*	*ZPE*	*E* + *ZPE*	E_{HOMO}	E_{LUMO}	ΔE
SO_3	-623.592685	0.012560	-623.580125	-10.0873	-2.67109	7.41625
CYCLIC	-623.489860	0.009880	-623.479980	-9.26990	-2.32605	6.94385
CIS	-623.447221	0.009880	-623.437341	-7.95912	-4.25210	3.70702
TRANS	-623.437669	0.009213	-623.428456	-7.80973	-4.59522	3.21451
SQUARE	-623.337799	0.009923	-623.327876	-7.03556	-3.84989	3.18567
TS1	-623.331323	0.009549	-623.321774	-6.47750	-3.70920	2.76830
TS2	-623.414837	0.008503	-623.406334	-7.73820	-4.94270	2.79550
TS3	-623.433429	0.008871	-623.424558	-8.85790	-6.89270	1.96520
TS4	-623.431820	0.008648	-623.423172	-7.73653	-4.75496	2.98157
TS5	-623.433428	0.008868	-623.424560	-8.85790	-6.89490	1.96300

While the hardness values of the transition states are less than the corresponding values of the ground state isomers, polarizability values are proved to be larger for the transition states as it would be expected. This behavior could be rationalized in terms of energy content where the transition states are more energetic.

Electric properties of SO₃ isomers

Linear and nonlinear optical properties in atomic units in addition to the estimated electric dipole moments of SO_3 isomers are listed in Table 5.

Table 5. TD-B3LYP/aug-cc-pV(Q+d)Z//PBE0/aug-cc-pV(Q+d)Z prediction of the electric properties of SO_3 isomers; dipole moment μ_e in *D*, average polarizability <α> in au, anisotropy Δα in au and average hyperpolarizabilities $\bar{\beta}$ and $\bar{\gamma}$ in au

Descriptor	SO_3	Cyclic	cis	trans	square
μ_e	0.0000	1.6958	3.2898	2.1547	1.3978
α_{xx}	32.220	35.244	36.649	69.537	35.057
α_{yy}	32.218	27.937	54.885	28.035	28.461
α_{zz}	20.505	28.324	23.258	23.366	36.245
<α>	28.314	30.502	38.264	40.313	33.254
Δα	11.451	7.121	27.497	44.022	7.263
β_x	-0.108	-124.7	210.0	100.4	377.5
β_y	0.000	-183.2	-316.9	285.8	-65.3
β_z	0.028	0.0	0.0	0.1	471.4
$\bar{\beta}$	0.112	221.6	380.1	302.9	607.4
γ_{xxxx}	2908.7	4577.2	4349.6	4081.5	4495.5
γ_{yyyy}	1574.8	4780.6	6226.1	6434.0	10658.4
γ_{zzzz}	2929.0	2738.1	2812.3	3115.3	5404.0
γ_{xxyy}	758.4	1503.8	2191.0	2603.7	2808.7
γ_{xxzz}	969.7	1364.5	1212.3	3005.6	2042.3
γ_{yyzz}	758.4	1462.7	3108.4	1510.0	3226.2
$\bar{\gamma}$	2473.4	4151.6	5282.1	5573.9	7382.4

Obviously, polarizability descriptors vary among the isomers, yet, with no apparent trend. On the other hand, hyperpolarizability invariants, $\bar{\beta}$ and $\bar{\gamma}$, reflected a regular change, in consistency with the isomers stability where the SO_3 (D_{3h}) isomer bears the minimum value of either $\bar{\beta}$ or $\bar{\gamma}$ and the maximum values are recorded for the least stable square isomer. Theoretical obtained values of static linear and nonlinear optical properties of these isomers could not be compared with the corresponding experimental or theoretical values due to lack of the corresponding experimental or theoretical values, according to the best of our knowledge. The only data that has been found is that of $<\alpha>$ of the D_{3h} global minima[43] where our calculated value is in great accordance with it.

While the trans isomer evidently provided the highest α_{xx} component (69.537 au) the cis one showed the maximum in α_{yy} (54.885 au). This behavior has reflected positively on $\Delta\alpha$, deviation from spherical symmetry, where it is relatively large for the cis and trans isomers (27.497 au and 44.022 au respectively). On the other hand $\Delta\alpha$ varied insignificantly in the case of D_{3h}, cyclic and square isomers. The relative increase of $<\alpha>$ relative to D_{3h} isomer: D_{3h} < cyclic (2.568 au) < square (5.320 au) < cis (10.330 au) < trans (12.3979 au).

Its found that the magnitude of $\bar{\beta}$ is zero for D_{3h} isomer. This behavior could be attributed to the high symmetry of the D_{3h} isomer where $\bar{\beta}$ value vanishes for high centro-symmetric structures. The other isomers showed tangible variation in $\bar{\beta}$ where the largest value ($\bar{\beta} = 607.4\,au$) has been noticed for the square isomer. We found that the relative increase in $\bar{\beta}$ relative to the D_{3h} isomer is: D_{3h} < cyclic (222 au) < trans (303 au) < cis (380 au) < square (607 au).

Calculations have shown that the SO_3 (D_{3h}) isomer displays the smallest $\bar{\gamma}$ value (2473.4 au) among all other isomers according to B3LYP/aug-cc-pV(Q+d)Z calculations. The maximum value of $\bar{\gamma}$ (7382.4 au) was found associated with the square isomer. The relative increase in $\bar{\gamma}$ according to our calculation with respect to that of the D_{3h} isomer is: D_{3h} < cyclic (1678 au) < cis (2809 au) < trans (3101 au) < square (4909 au).

Global minimum SO_3 (D_{3h}) isomer

Vibrational contribution to the $\tilde{X}\,^1A_1$ ground state of SO_3 (D_{3h})

It is well known that vibrational contributions to polarizabilities can be significant[45]. Additionally, the electric property derivatives are of major importance in spectroscopic investigations. Whereas dipole polarizability derivatives find applications in estimation of vibrational intensities[46], non linear hyperpolarizability derivatives are associated with vibrational hyper-Raman intensities[47]. In order to make estimation, anisotropy and dipole polarizability principal components ($R-R_e$) dependence were investigated with respect to the symmetric S = O bond length change (R) around the equilibrium bond distance (R_e) at the PBE0/aug-cc-pV(Q+d)Z level of theory. We found that Cartesian components, average molecular polarizability and anisotropy are smoothly varied as it is depicted in Figure 4. Besides, the longitudinal polarizability component α_{xx} varies more rapidly with S = O symmetric stretching than the transversal one α_{zz}. R-dependence of the invariants of the linear optical polarizability around R_e is conveniently represented by the equations:

$$<\alpha>_{(R)} / e^2 a_o^2 E_h^{-1} = 0.476(R - R_e)^4 - 2.985(R - R_e)^3 + 5.013(R - R_e)^2 + 22.416(R - R_e) + 28.19$$

$$\Delta\alpha_{(R)} / e^2 a_o^2 E_h^{-1} = -3.66(R - R_e)^4 - 1.457(R - R_e)^3 + 10.650(R - R_e)^2 + 19.764(R - R_e) + 11.786\,A$$

numerical fit of both the first and the second derivatives of polarizability invariants gave

$\left(\dfrac{d^n <\alpha>}{dR^n}\right)_e$ for $n = 1,2$ are $22.146\,e^2a_o^2E_h^{-1}$ and $10.026\,e^2a_o^2E_h^{-1}$ while those of $\left(\dfrac{d^n (\Delta\alpha)}{dR^n}\right)_e$ are

$19.764\,e^2a_o^2E_h^{-1}$ and $21.300\,e^2a_o^2E_h^{-1}$ respectively. Similar calculations have been conducted with the B3LYP functional with the same basis set and the following results have been obtained:

$<\alpha>_{(R)} /e^2a_o^2E_h^{-1} = 0.004(R - R_e)^4 - 2.599(R - R_e)^3 + 4.835(R - R_e)^2 + 22.651(R - R_e) + 28.963$

$\Delta\alpha_{(R)} / e^2a_o^2E_h^{-1} = -0.788(R - R_e)^4 - 2.737(R - R_e)^3 + 9.339(R - R_e)^2 + 20.970(R - R_e) + 12.273$

$\left(\dfrac{\partial <\alpha>}{\partial R}\right)_e = 22.651\,e^2a_o^2E_h^{-1}, \qquad \left(\dfrac{\partial (\Delta\alpha)}{\partial R}\right)_e = 20.970\,e^2a_o^2E_h^{-1}, \qquad \left(\dfrac{\partial^2 <\alpha>}{\partial R^2}\right)_e = 9.67\,e^2a_o^2E_h^{-1}$ and

$\left(\dfrac{\partial^2 (\Delta\alpha)}{\partial R^2}\right)_e = 18.678\,e^2a_o^2E_h^{-1}.$
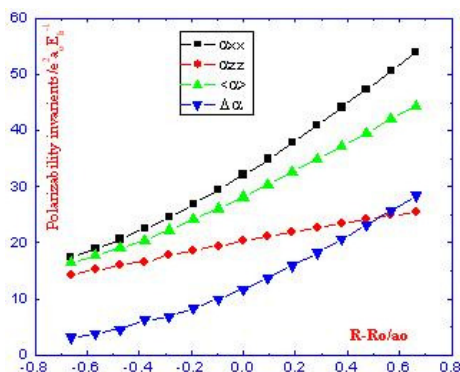
Figure 4. Dependence of polarizability invariants on $S = O$ symmetric stretch as predicted by PBE0/aug-cc-pV(Q+d)Z level of theory

Excited states of $SO_3 (D_{3h})$

Excited states were modeled in this work by CIS and CIS(D) models. In CIS[37], we consider every possible single excitation that can be formed by excitation from the electronic ground state of doubly occupied orbital to the virtual orbital. Inner shells are usually frozen for this procedure.

The CIS(D)[38], which is a perturbation treatment based on CIS model, was proposed as a correction to CIS through the introduction of the effect of double substitutions into the CIS wave function. One performs the CIS calculations and then add the CIS(D) correction to the excitation energies.

Transition intensity from a ground state (*g*) to an excited one (*e*) has been expressed in this work in terms of oscillator strength f_{eg}

$$f_{eg} = \left(\frac{4\pi m_e}{3e^2h}\right) v_{eg} \left|\mu_{eg}\right|^2 \qquad (9)$$

Where v_{eg} is the excitation frequency, μ_{eg} is the transition dipole moment such that $\mu_{eg} = \langle e|\mu|g\rangle$ and the remaining components are the usual physical constants. The oscillator

strength could be expressed in terms of the wave number $\bar{v}_{eg}$ in cm^{-1} and debye units in case of the transition dipole moment as the following[48] $f_{eg} = 4.70165 \times 10^{-7} cm\, D^{-2} \bar{v}_{eg} |\mu_{eg}|^2$. Oscillator strength in addition to the estimated CIS and CIS(D) energies of the selected excited states are recorded in Table 6.

Table 6. Vertical excitation energy and oscillator strength of each of the selected excited states of the D_{3h} isomer as it is predicted by CIS and CIS(D)/aug-cc-pV(Q+d)Z

State	contribution	f_{eg}	ε_{CIS}/eV	$\varepsilon_{CIS(D)}/eV$
$1\,^3A_1''$	$11a_1^2 \rightarrow 12a_1^0$	0.0000	6.2295	5.3299
$1\,^3A_2'$	$6b_1^2 \rightarrow 12a_1^0$	0.0000	6.3559	6.6940
$2\,^3A_2'$	$1a_2^2 \rightarrow 12a_1^0$	0.0000	6.3566	6.6850
$3\,^3A_2'$	$11a_1^2 \rightarrow 4b_2^0$	0.0000	6.6868	4.8242
$3\,^3A_1''$	$6b_1^2 \rightarrow 4b_2^0$	0.0000	7.2273	6.5740
$2\,^1A_1''$	$11a_1^2 \rightarrow 12a_1^0$	0.0000	6.7318	5.5104
$9\,^1A_1''$	$6b_1^2 \rightarrow 12a_1^0$	0.0252	8.7826	7.5105
$10\,^1A_1''$	$1a_2^2 \rightarrow 12a_1^0$	0.0251	8.7835	7.5108
$9\,^1A_2'$	$5b_1^2 \rightarrow 4b_2^0$	0.2513	10.1584	8.0672
$10\,^1A_2'$	$10a_1^2 \rightarrow 4b_2^0$	0.2518	10.1599	8.0670

Geometry of excited states of SO$_3$ (D$_{3h}$)

Table 7 presents various bond distances R in pm, bending angles and Mulliken charges of the selected triplet and singlet excited states. In general, insignificant changes in geometrical parameters were found among the triplet and the singlet excited states. This could be attributed to the high symmetrical D_{3h} parent isomer and retention of centro-symmetric geometry of the selected excited states.

Table 7. Geometrical parameters of the selected excited states as it is predicted by CIS and CIS(D)/ aug-cc-pV(Q+d)Z level of theory**;** where R is the bond distance in pm, $\angle$ is the bending angle in degree and Q is the charge in coulomb

Parameter	$1\,^3A_1''$	$2\,^3A_2'$	$3\,^3A_2'$	$2\,^1A_1''$	$9\,^1A_1''$	$10\,^1A_1''$	$10\,^1A_2'$
$R_{S-O(3)}, R_{S-O(4)}$	144.7	145.3	144.3	144.7	144.2	144.1	144.2
$R_{S-O(2)}$	144.7	151.0	144.3	144.7	156.0	156.0	156.0
$\angle_{O(3)SO(2)}$	120.0	115.4	120.0	120.0	116.8	116.9	116.8
$\angle_{O(3)SO(4)}$	120.0	129.2	120.0	120.0	126.3	126.3	126.3
Q_S	2.260	1.6011	2.265	2.260	2.214	2.21	2.214
$Q_{O(3)}, Q_{O(4)}$	-0.753	-0.755	-0.755	-0.753	-0.747	-0.747	-0.747
$Q_{O(2)}$	-0.753	-0.737	-0.755	-0.753	-0.719	-0.719	-0.719

Electric properties of the excited states of SO_3 (D_{3h})

Linear and nonlinear optical susceptibilities of the excited states calculated at CIS/aug-cc-pV(Q+d)Z level of theory utilizing Firefly are provided in Table 8. While these states show relative similarity in terms of polarizabilities and first order hyperpolarizabilities in the case of reported singlet and triplet excited states, they slightly differ in the second order hyperpolarizability invariant. The differences become more pronounced in the anisotropic calculations $\Delta_1\gamma$ and $\Delta_2\gamma$; $\Delta_1\gamma=3\gamma_{zzzz}-4\gamma_{xxxx}+3\gamma_{xxzz}$ and $\Delta2\gamma=\gamma_{zzzz}+\gamma_{xxxx}-6\gamma_{xxzz}$[49]

To the contrary, excited states of each of the angular triatomic molecules SO_2, O_3 and NO_2[23,50,51], with C_{2V} point group of each have reflected substantial differences in terms of geometrical structures and symmetrical point group. Each excited state of these prototype molecules has a definite linear and NLO properties differ from that of the others.

Table 8. The static linear and nonlinear optical properties of the given excited states in au as calculated by the TD-B3LYP/aug-cc-pV(Q+d)Z//CIS/aug-cc-pV(Q+d)Z level of theory

Parameter	$1\,^3A_1''$	$1\,^3A_2'$	$2\,^3A_2'$	$3\,^3A_2'$	$9\,^1A_1''$	$10\,^1A_1''$	$10\,^1A_2'$	$10\,^1A_2''$
α_{xx}	33.78	35.79	35.80	33.53	35.07	36.058	35.11	35.07
α_{yy}	33.78	34.73	34.74	33.53	36.40	21.390	21.40	36.40
α_{zz}	20.79	21.23	21.23	20.71	21.39	35.399	36.38	21.39
$<\alpha>$	29.45	30.58	30.60	29.26	30.95	30.949	30.96	30.95
$\Delta\alpha$	9.19	9.94	9.95	9.07	10.17	10.147	10.18	10.17
β_x	0.00	0.06	0.08	-0.01	0.05	-6.102	-1.05	0.05
β_y	0.01	-22.61	-21.75	0.04	7.09	0.000	0.00	7.09
β_z	0.00	0.00	0.00	0.00	0.00	3.472	7.01	0.00
$\overline{\beta}$	0.01	21.60	21.76	0.04	7.09	7.020	7.08	7.09
γ_{xxxx}	2729	2710	2711.0	2758.8	2702.7	3212.6	2727.8	2703.3
γ_{yyyy}	2783	3075	3075.4	2759.0	3236.5	1636.2	1637.3	3236.1
γ_{zzzz}	1445	1561	1561.2	1431.6	1636.3	2944.8	3239.3	1636.1
γ_{xxyy}	927	1079	1079.1	919.66	1086.8	784.6	703.9	1086.6
γ_{xxzz}	687	699	699.5	919.7	701.1	977.3	1074.9	701.2
γ_{yyzz}	6687	774	774.4	680.8	812.4	728.8	810.5	812.3
$\overline{\gamma}$	2322.9	2490	2490.8	680.9	2555.2	2555.0	2556.6	2555.1
$\Delta_1\gamma$	-4517	-4060	-4062	-3981	-3799	-1084.1	2031.4	-3801.3
$\Delta_2\gamma$	49.8	74.9	75.2	-13275	132.4	293.6	-482.3	132.2

Conclusion

In the present study, ground and excited states of sulfur trioxide have been investigated with the expensive PBE0/aug-cc-pV(Q+2df)//PBE0/aug-cc-pV(Q+d)Z level of theory using Gaussian 09, PCGAMESS, MOLEKEL and AIM2000 packages. Four different local minima geometrical structures in addition to the global minima D_{3h} isomer were located on the potential energy surface. Molecular surface electrostatic potential and bond critical point calculations showed that $V_{S,min}$ and $V_{S,max}$ are located at the oxygen and sulfur sites respectively. Linear and nonlinear optical properties and hardness of the titled isomers calculations lead to the observation that the state of minimum polarizability, hyperpolarizabilities and maximum hardness are associated with the geometry of minimum

energy content. The PBE0/aug-cc-pV(Q+d)Z dipole polarizability and anisotropy variation around R_e is adequately presented by Taylor expansion. The striking features regarding the triplet and singlet excited states are that of similarity in both geometrical and electronic parameters at the level of theory employed in this investigation.

References

1. Barber J, Chrysostorm E T H, Masiello T, Nibler J W, Maki A, Weber A, Blake T A and Samsm R L, *J Mol Spectrosc.,* 2002, **216(1)**, 105-112.
2. Barber J, Chrysostorm E T H, Masiello T, Nibler J W, Maki A, Weber A, Blake T A and Samsm R L, *J Mol Spectrosc*., 2003, **218(2)**, 197-203.
3. Barber J, Chrysostorm E T H, Masiello T, Nibler J W, Maki A, Weber A, Blake, T. A and Samsm R L, *J Mol Spectrosc,* 2003, **218(2)**, 204-212.
4. Sharpe S W, Blake T A, Sams R L, Maki A, Masiello T, Barber J, Vulpanovici N, Nibler J W and Weber A, *J Mol Spectrosc,* 2003, **222(2)**, 142-152.
5. Palmer K J, *J Am Chem Soc.,* 1938, **60(10)**, 2360-2369.
6. Gillespie R J and Hargihai I, The VSEPR Model of Molecular Geometry, Courier Corpotation:2nd Ed., USA, 2012, 133-135.
7. Henfrey N F and Thrush B A, *Chem Phys Lett.,* 1983, **102(2-3)**, 135-138.
8. Clark A H and Beagley B, *Trans Faraday Soc.,* 1971, **67**, 2216-2224.
9. Dorney A J, Hoy A R and Mills I M, *J Mol Spectrosc.,* 1973, **45(2)**, 253-260.
10. Ortigoso J, Escribano R and Maki A G, *J Mol Spectrosc.,* 1989, **138(2)**, 602-613.
11. Masiello T, Barber J, Chrysostorm E T H, Nibler J W, Maki A, Weber A, Blake T A and Sams R L, *J Mol Spectrosc.,* 2004, **223(1)**, 84-95.
12. Chrysostorm E T H, Vulp-anovici N, Masiello T, Barber J, Nibler J W, Weber A, Maki A and Blake T A, *J Mol Spectrosc.,* 2001, **210(2)**, 233-239.
13. Martin J M L, *Spectrochemica Acta A Molecular Biomolecular Spectroscopy,* 1999, **55(3)**, 709-718.
14. Martin J M L, *Chem Phys Lett.,* 1999, **310(3-4)**, 271-276.
15. Jou S H, Shen M Y, Yu C H and Lee Y P, *J Chem Phys.,* 1996, **104**, 5745-5753.
16. Bondybeg V E and English J H, *J Mol Spectrosc.,* 1985, **109(2)**, 221-228.
17. Burkholder J B and Mckeen S, *Geophys Res Lett.,* 1997, **24(24)**, 3201-3204.
18. Hintze P E, Kjaergaard H J, Vaida V and Burkholder J B, *J Phys Chem A,* 2003, **107(8)**, 1112-1118.
19. Nelson R M and Smyth W D, *Icarus.,* 1986, **66(1)**, 181-187.
20. Young L and Young A, *Sc Am.,* 1975, **233(3)**, 70-78.
21. Cotton F A and Wilkinson G, Advanced Inorganic Chemistry; 4th Ed., Wiley: New York, 1980, 529-530.
22. Robinson T W, Schofield D P and Kjaergaard H G, *J Chem Phys.,* 2003, **118**, 7226-7232.
23. Soscún H, Hernández J, Escobar R, Toro-Mendoza Ć, AlvaradoY and Hinchliffe A, *Int J Quant Chem.,* 2002, **90(2)**, 497-506.
24. Korambath P P and Karna S P, *J Phys Chem A,* 2000, **104(20)**, 4801-4804.
25. Parr R G and Pearson R G, *J Am Chem Soc.,* 1983, **105**, 7512-7516.
26. Chattaraj P K, Fuentealba P, Gomez B and Contreras R, *J Am Chem Soc.,* 2000, **122**, 348-351.
27. Hinchliffe A, Mkadmh A, Machado H J S and Abu-Awwad F M, *J Mol Struct Theochem.,* 2005, **717(1-3)**, 231-234.
28. Becke A D, *J Chem Phys.,* 1993, **98(7)**, 5648-5652.

29. Lee C, Yang W and Parr R G, *Phys Rev B*, 1988, **37(2),** 785-789.
30. Perdew J P, Burke K and Ernzerhof M, *Phys Rev Lett.,* 1996, **77(18)**, 3865-3868.
31. Perdew J P, Burke K and Ernzerhof M, *Phys Rev Lett.,* 1997, **78**, 1396.
32. Adamo C and Barone V, *J Chem Phys.,* 1998, **108**, 664-675.
33. Vosko S H, Wilk L and Nusair M, *Can J Phys.,* 1980, **58(8)**, 1200-1211.
34. Cohen H D and Roothan C C J, *J Chem Phys.,* 1965, **43**, S34-S38.
35. Dunning Jr T H, Peterson K A and Wilson A K, *J Chem Phys.,* 2001, **114**, 9244-9253.
36. Biegler-König F, Bayles D and Schönbohm J, *J Comp Chem.,* 2001, **22(5)**, 545-559.
37. Foresman J B, Head-Gordon M, Pople J A and Frisch M J, *J Phys Chem.,* 1992, **96(1)**, 135-149.
38. Head-Gordon M, Rico R J, Oumi M and Lee T J, *Chem Phys Lett.,* 1994, **219(1-2)**, 21-29.
39. Granovsky A A Firefly version 7.1.G, http://classic.chem.msu.su/gran/firefly
40. Mulliken R S, *J Chem Phys.,* 1955, **23**(10), 1833-1840.
41. Frisch M J, Gaussian 09, Revision A.03; Gaussian, Inc., Wallingford CT, 2009.
42. Bell R D and Wilson A K, *Chem Phys Lett.,* 2004, **394(1-3)**, 105-109
43. Nagarajan G, Lippincott E R and Stutman J M, *J Phys Chem.,* 1965, **69(6)**, 2017-2021.
44. Varetto U, MOLEKEL 5.4; Swiss National Supercomputing Centre; Manno, Switzerland.
45. Haskopoulos A and Maroulis G, *Chem Phys Lett.,* 2004, **397(1-3)**, 253-257.
46. Tang J and Albrecht A C, In Raman Spectroscopy; Szymanski H.A, Eds., New York, 1970, **2**, Chap. 2.
47. Yang W H and Schatz G C, *J Chem Phys.,* 1992, **97(5)**, 3831-3845.
48. Kjaergaard H G, Yu H, Schattka B J, Henry B R and Allan W T, *J Chem Phys.,* 1990, **93(9)**, 6239-6248.
49. Maroulis G, *Chem Phys.,* 2003, **291**, 81-95.
50. Hinchliffe A, Mkadmh A, Soscun H J and Abu-Awwad F M, *Int J Appl Chem.,* 2005, **1(1)**, 71-83.
51. Hinchliffe A, Humberto J S, Mkadmh A, and Abu-Awwad F M, *J Comp Methods Sci Eng.,* 2006, **6**(**1-4)**, 165-170.